

## 8.1 DEVELOPMENT OF A CLIMATOLOGY OF VERTICALLY COMPLETE WIND PROFILES FROM DOPPLER RADAR WIND PROFILER SYSTEMS

Robert E. Barbré, Jr.  
Jacobs ESSSA

### 1. INTRODUCTION

Space vehicle loads and trajectory assessments utilize archives of both discrete and sequential wind profiles to ensure robust structural integrity during vehicle design. Historically, vehicle programs have used balloon-based measurements, which have three primary limitations inherent to balloon systems. First, the high cost of balloon releases makes high-frequency balloon sampling impractical, thereby limiting sample size of archives and thus increasing statistical uncertainty in vehicle ascent analyses. Second, historical vehicle program requirements have influenced the temporal interval of day-of-launch (DOL) balloon measurements, which constrains the intervals that current vehicle programs can assess wind change. Third, balloon measurements could misrepresent the environment through which the vehicle flies due to downrange drift and rise time characteristics. The Marshall Space Flight Center Natural Environments Branch (MSFC NE) developed an archive of quality controlled (QC'ed) wind profiles from Kennedy Space Center's (KSC's) 50-MHz Doppler Radar Wind Profiler (DRWP) system (Decker and Barbré 2011, Barbré 2012) to mitigate these shortcomings as the DRWP archive provides orders of magnitude more profiles than balloon archives and allows for wind change assessments over numerous time intervals. In addition, the near-instantaneous and near-vertical sampling of a DRWP profile theoretically represents the wind through a vehicle's flight path better than a drifting balloon. NASA's Ares and Space Launch System (SLS) launch vehicle programs have incorporated the DRWP in the early design phase. However, the 50-MHz DRWP archive contains a limitation in that it does not contain data below 2.7 km, which left MSFC NE with the desire to merge the 50-MHz DRWP output with that from other DRWP systems to support any application that may require characterizing wind magnitudes and changes at these low altitudes.

MSFC NE develops a technique to generate vertically-complete DRWP wind profiles using the previously-generated 50-MHz DRWP archive (Barbré 2012) and an archive from the 915-MHz DRWP network at the United States Air Force Eastern Range (ER) to provide the capability to assess the wind's effects on the vehicle at low altitudes. Applications that require knowledge of winds below 2.7 km include liftoff clearance, plume damage, and crew capsule pad abort.

MSFC NE leverages on the 915-MHz DRWP systems

at the ER to produce wind profiles that start near the Earth's surface with a similar temporal frequency as the 50-MHz DRWP archive. After determining that the available 915-MHz DRWP archive should produce enough wind data that would reach the minimum measurement altitude of the 50-MHz DRWP (Murri 2011), MSFC NE performed an extensive QC evaluation on the 915-MHz DRWP archive similar to Barbré (2012). Then, concurrent output from both DRWP sources were merged to produce wind profiles extending from roughly 0.2-18.5 km over the 2000-2009 period of record (POR). The paper herein summarizes the 50- and 915-MHz DRWP systems and archives, the QC and splicing process, validation analyses, and the resultant database's attributes.

### 2. DRWP DESCRIPTIONS

#### 2.1 50-MHz DRWP

Although documentation of the 50-MHz DRWP hardware and data processing algorithm exists (Merceret 1997, Schumann et al. 1999, Barbré 2012), this section provides an overview as well as the 50-MHz DRWP's data attributes. The 50-MHz DRWP is located just east of the Shuttle Landing Facility at KSC, and consists of an irregular octagon-shaped antenna field, which spans 15,600 m<sup>2</sup> and consists of coaxial-collinear elements set 1.5 m above the ground plane made of copper wire. These elements send electronic pulses at 49.25 MHz through three beams. One beam points vertically, and two oblique beams point 15° off zenith at azimuths of 45° and 135° east from north. All beams have a 3° beam width (Merceret 2000). Figure 1 presents a photograph of the 50-MHz DRWP antenna field along with the adjacent trailer that stores the radar's electronics. One should note that a new 50-MHz DRWP with different hardware and beam characteristics has replaced this instrument.



**Figure 1:** Photograph of the KSC 50-MHz DRWP and trailer (courtesy of F. Merceret).

---

\*Corresponding Author Address: Robert E. Barbré, Jr., Jacobs ESSSA, 1500 Perimeter Pkwy, Huntsville, AL; 35806; email: [robert.e.barbre@nasa.gov](mailto:robert.e.barbre@nasa.gov).

To measure wind velocities, the 50-MHz DRWP sends radio pulses in three beam directions sequentially and measures the return signal through Bragg Scatter at wavelengths scaling to roughly 3 m (Rinehart 2004). A Fast Fourier Transform converts the signal to Doppler power spectra over 256 frequency bins at each range gate. In the beginning of the POR, 112 range gates exist from 2,011-18,661 m every 150 m. After an upgrade (Pinter et al. 2006) in July – August 2004, 111 range gates exist from 2,666-18,616 m every 145 m. Also before this upgrade, profiles exist every five minutes. After the upgrade, profiles exist every three minutes. After obtaining the Doppler spectra for each beam, the 50-MHz DRWP's post processing algorithm computes radial velocities using the Median Filter First Guess (MFFG) algorithm (Schumann et al. 1999), which applies to the horizontal beams only as the post processing does not use the vertical beam to calculate horizontal winds (Schumann et al. 1999, Wilfong et al. 1993). Horizontal winds are then computed using triangulation of the oblique beams' radial velocities. This algorithm produces a wind speed estimate regardless of the backscattered signal by propagating the FG velocity if necessary. Therefore, a complete profile exists at every timestamp in the non-QC'ed 50-MHz DRWP archive.

Although the MFFG algorithm has many advantages over the traditional consensus averaging technique used on other wind profilers (Schumann et al. 1999), using the algorithm does not completely prevent acquiring erroneous data. In many instances, the FG simply associates itself with spectral peaks that do not represent the real wind. Other instances of suspect data occur when the signal is too weak to calculate a radial velocity, within ground clutter, or during convective events. The latter characteristic tends to violate the homogenous atmosphere assumption used in the horizontal wind computation.

MSFC NE has archived 50-MHz DRWP output over the 1997-2009 POR. In addition to the computed horizontal wind speed (WS), wind direction (WD), and altitude (z); spectral width (SW), signal power, noise level, vertical velocity ( $w$ ), number of FGPs, and an internal shear value ( $s^{-1}$ ) at each gate exist. The QC process computes the westerly ( $u$ ) and southerly ( $v$ ) wind components from WS and WD. Table 1's second column provides attributes of MSFC NE's 50-MHz DRWP archive.

## 2.2 915-MHz DRWP

As with the 50-MHz DRWP, documentation that provides detailed descriptions of the ER 915-MHz DRWP network exist (Lambert et al. 2003, 45<sup>th</sup> Space Wing 2013, Lambert and Taylor 1998), but the paper provides an overview here for convenience. The United States Air Force owns the 915-MHz DRWP network, which consists of five 915-MHz DRWPs arranged in a diamond-shaped pattern around the periphery of the ER. Figure 2 displays the locations of each 915-MHz DRWP and the 50-MHz DRWP. The Mosquito Lagoon (ML) DRWP is located in thick vegetation on the northern side of the ER, and is closest to the 50-MHz DRWP. The False Cape (FC)

**Table 1:** Attributes of the KSC 50- and 915-MHz DRWP, as well as the parameters used in the QC process for each system.

	KSC 50-MHz	KSC 915-MHz
Period of Record	08/1997-12/2009	04/2000-12/2010
Measurement	MFFG	Consensus Avg.
Approximate Sampling Rate	3-5 minutes	12-15 minutes
Approximate Altitude Range	2,500-18,500 m	200-6,100 m
Approximate Altitude Interval	145 m	100 m
<b>Parameters In Output File</b>		
Wind Speed	X	X
Wind Direction	X	X
Vertical Velocity	X	X
Radial Velocity		X
SNR	X	X
Radial Shear	X	
Spectral Width	X	
First Guess Propagations	X	
Consensus Avg. Time and Records		X
<b>Computed Parameters</b>		
U	X	X
V	X	X
DU vs. Time	X	X
DV vs. Time	X	X
Shear	X	X
Convection Flag	X	X

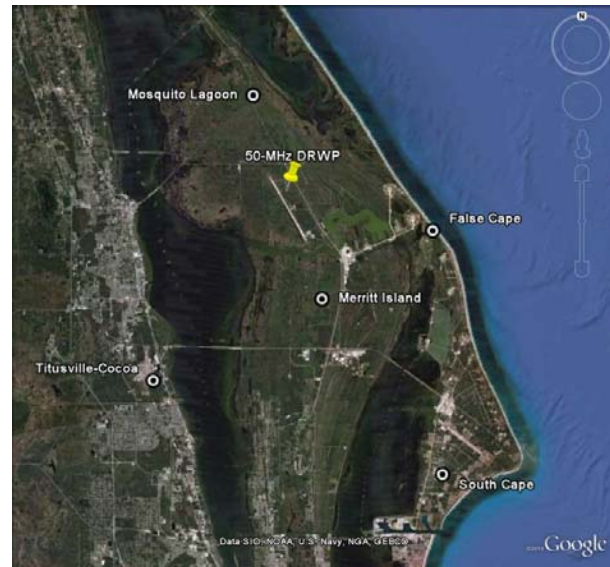


**Figure 2:** Google Earth image of the ER DRWP network.

DRWP is located closest to shore and near Launch Complex 39. The South Cape (SC) DRWP is located in the industrial area within the southern part of the ER. The Merritt Island (MI) DRWP is located in the middle of the ER in a heavily vegetated region between the Banana and Indian Rivers. Finally, the Titusville-Cocoa (TC) DRWP is located at the Titusville-Cocoa airport, which is within a relatively urban region and furthest inland. The network's configuration allows for each 915-MHz DRWP to potentially sample a different atmospheric boundary

layer regime, especially in a dynamic environment. Thus, an individual 915-MHz DRWP's location contributes to that DRWP's influence in wind analyses relating to space vehicles.

An individual 915-MHz DRWP measures atmospheric motions in a very similar manner to the 50-MHz DRWP with some different configurations. Each 915-MHz DRWP is a standard Radian model LAP 3000 915-MHz DRWP with proprietary LAP-XM software (Radian International 2001). Some differences from the 50-MHz DRWP include an 8° beam width, signal attenuating at lower altitudes, and the much smaller physical size (Figure 3). A 915-MHz DRWP has an aperture of 6 m<sup>2</sup> (45<sup>th</sup> Space Wing 2013) as opposed to the 15,600 m<sup>2</sup> aperture of the 50-MHz DRWP (Schumann et al. 1999). Similar to the 50-MHz DRWP, Bragg scatter produces the return signal, but at wavelengths scaling to roughly 0.2 m. In addition, the 915-MHz DRWP can use up to four oblique beams, which the configuration orients to minimize ground clutter effects at the radar's site. However, the instrument uses only two oblique beams to measure winds in order to maximize horizontal resolution (Lambert and Taylor 1998), and all 915-MHz DRWPs used a three-beam configuration with the oblique beams generally pointing north and east during the POR.



**Figure 3:** Picture of a 915-MHz DRWP at the ER (bottom, 45<sup>th</sup> Space Wing 2013).

Perhaps the most significant difference exists in the signal postprocessing algorithm that generates radial velocities. Unlike the 50-MHz DRWP which uses the MFFG algorithm, the 915-MHz DRWP uses a consensus-averaging technique to process the return signal (Lambert et al. 2003, 45<sup>th</sup> Space Wing 2013, Lambert and Taylor 1998). This technique produces a wind record that ideally represents an 11- to 14-minute average wind. Triangulation also produces horizontal winds from radial velocities, but incorporates the vertical velocity if enough records exist from the vertical beam to create a consensus. This triangulation also assumes a homogeneous wind environment across the distance DRWP's configurations nominally provide measurements spanning the input oblique beams. The 915-MHz DRWP's output altitudes range from either 87-4,438 m or

from 130-6,100 m, approximately every 101 m. The maximum altitude of an individual 915-MHz DRWP profile varies significantly because the consensus-averaging algorithm does not produce a wind record in cases where a weak backscattered signal exists. As a result, not all altitudes in the 915-MHz DRWP archive contain wind data. Additionally, the consensus-averaging algorithm does not remove spurious signals as effectively as the MFFG (Wilfong et al. 1993), and provides measurements on a coarser temporal scale.

MSFC NE obtained the 915-MHz DRWP archive from KSC's Tropical Rainfall Measurement Mission (TRMM) website (<http://trmm.ksc.nasa.gov>) for the April 2000 to December 2010 POR. An individual file first consists of metadata for a profile, followed by z, WS, WD, each beam's radial velocity, number of records in consensus window, and SNR at each altitude. MSFC NE obtained the archive from the TRMM website because MSFC NE's archive does not start until 2007. Thus, the TRMM 915-MHz DRWP archive made this work possible because without it, MSFC NE would not have enough data to use in statistical analyses. Table 1's third column provides attributes of the 915-MHz DRWP archive.

MSFC NE performs a rigorous QC process to the 915-MHz DRWP archive that heavily references work previously performed on the 50-MHz DRWP (Barbré 2012) and on a smaller sample of 915-MHz DRWP data (Lambert and Taylor 1998, Lambert et al. 2003). MSFC NE QC'ed data through 2009 to coincide with the end of the 50-MHz DRWP archive. Thus, the POR of the database that this paper describes extends from April 2000 through December 2009.

### 3. DATA QUALITY CONTROL PROCESS

The processes MSFC NE implements to QC the 50- and 915-MHz DRWP databases mimic what has been done in the literature, but contain some unique attributes based on data examination where appropriate. The QC processes for both archives consist of automated and manual checks, and removes flagged data before implementing the next check. The QC process assigns a flag to each check, and assigns the appropriate QC flag identifier if data from a particular time and altitude fail a given check. This section describes in detail the QC sequence for the 50- and 915-MHz DRWP individually. One should note that Barbré (2012) documents the 50-MHz DRWP QC process, but no such documentation exists for the 915-MHz DRWP QC process.

#### 3.1 Data Display System

MSFC NE develops graphical user interfaces (GUIs) to implement the QC process on both the 50- and 915-MHz DRWP data. Each GUI contains various functions to perform all QC procedures and save the desired output from a given DRWP system. Figure 4 shows an image of the GUI used in the 915-MHz DRWP QC process. The read function for the QC process scrutinizes data during each day sequentially and initially examines time-height

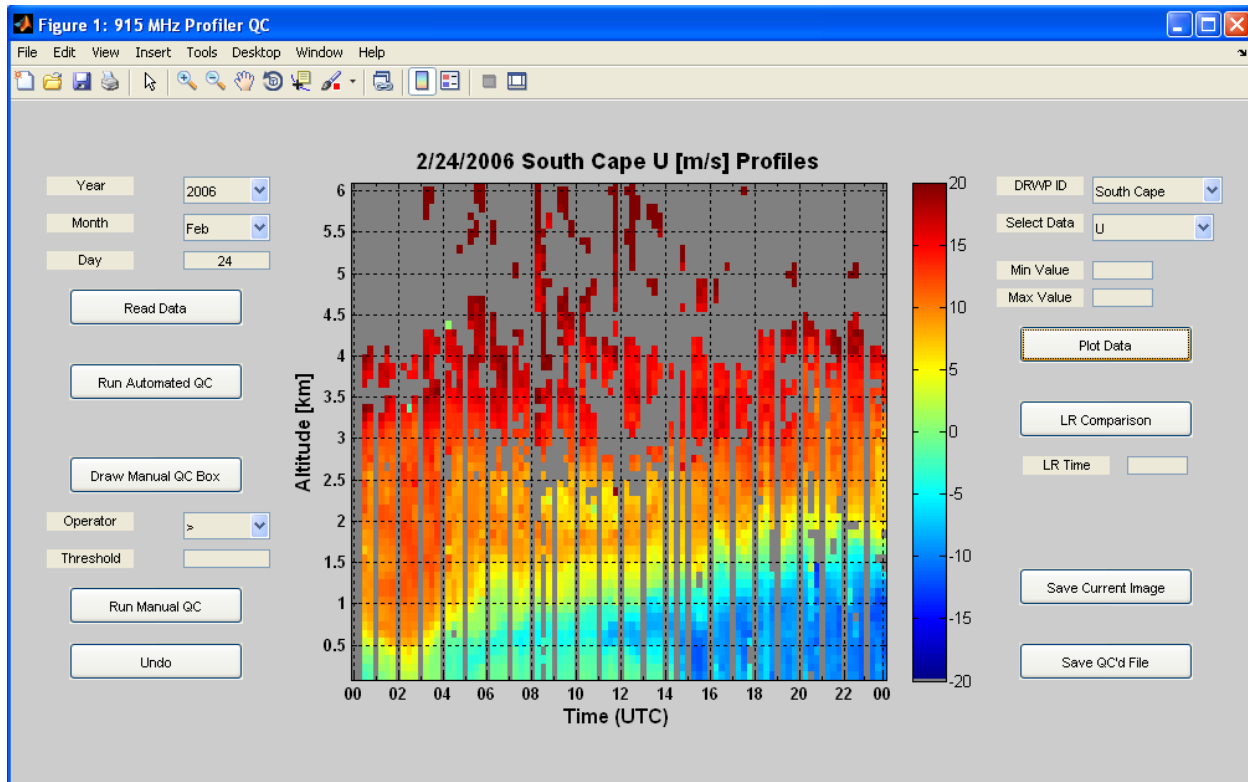


**Figure 4:** GUI used in the 915-MHz DRWP QC process.

sections of the meteorological and radar parameters shown in Table 1. The process then implements the automated QC and displays a new time-height section of the given variable. To perform the manual QC, the user draws a box surrounding the data in question and the algorithm removes data that the threshold flags. An “undo” function exists to protect against operator error during the manual QC process. Finally, the process saves the QC’ed file and manual QC logs. In addition, one can compare profiles from low-resolution (LR) weather balloons and the DRWP at a desired time, and save images as desired. The LR balloon database consists of rawinsondes prior to October 2002 and the Automated Meteorological Profiling System low-resolution flight element (Leahy and Overbey 2004) after October 2002. The general processes for the 50-MHz DRWP and 915-MHz DRWP greatly resemble each other; with the only significant difference consisting of manually inspecting each 915-MHz DRWP during a given day.

### 3.2 Automated Quality Control Process

The automated portion of the 50-MHz DRWP QC process contains procedures to fill data gaps and screen the vertical beam prior to removing horizontal winds. This procedure ensures a data record at least once every six minutes throughout the POR. The algorithm then screens the vertical beam without removing any data from the oblique beams or horizontal winds since the 50-MHz DRWP postprocessing does not use the vertical beam to calculate horizontal winds and the QC algorithm could

falsely flag a valid wind measurement that coincides with an erroneous vertical beam measurement. Checks are performed against the vertical beam’s signal, noise, and SW. In addition, a check exists to account for a systematic error that occurs when the vertical beam’s Doppler shift remains near zero (F. Merceret and B. Gober 2009, personal communication). This error appears when abnormally high  $|w|$  coincides with relatively low SNR. For this check, the algorithm calculates SNR including the signal below the noise level. Table 2 provides all of the thresholds that the 50-MHz DRWP automated QC process uses.

**Table 2:** Automated QC thresholds for the 50-MHz DRWP QC process.

QC Check	Threshold
Vertical SW*	$> 3.0 \text{ m/s}$
Vertical 0 Doppler Shift*	$ w  > 1.5 \text{ m/s}$ and Vertical SNR $< 40 \text{ dB}$
Vertical Signal or Noise*	Missing
Unrealistic Wind	$WS < 0 \text{ m/s}$ , $WD < 0^\circ$ , or $WD > 360^\circ$
East or North SW	$> 3.0 \text{ m/s}$
DRWP Shear	$> 0.1 \text{ s}^{-1}$
$ w $	$> 2.0 \text{ m/s}$
FGP	See Text
Meteorological shear	$> 0.1 \text{ s}^{-1}$
Small Median	See Text
East or North Signal	Missing
Rain / Convection	See Text
Isolated Datum	See Text

\* Denotes that the process only removes data from the vertical beam

Thresholds provide the basis of several automated checks, and the QC process first utilizes previous 50-MHz DRWP research (Merceret 1997, Carr et al. 1995), and modifies criteria if necessary based on data examination. After detecting physically unrealistic wind reports, the process examines the oblique beam SW to ensure that a wind report represents the environment within the sample volume and to validate the homogeneity assumption used to calculate the winds. The DRWP shear denotes the change in radial velocity per unit altitude and can detect large objects in the air such as airplanes (Merceret 1997). Very small vertical velocities generally exist over Florida in the altitude region that the 50-MHz DRWP samples, so any large perturbation in  $w$  indicates some anomaly in the air flow or that the 50-MHz DRWP is measuring the velocity of raindrops instead of the air. The threshold that this process uses provides a stricter criterion than Merceret (1997) because the original threshold does not flag many convective situations, especially after August 2004. The meteorological shear check serves the same purpose as the 50-MHz DRWP shear check but it applies to  $u$  and  $v$ . Missing signal power indicates that the 50-MHz DRWP does not contain a signal at that gate. Note that no check exists for the oblique beam noise level. An analysis was performed which shows that missing noise values have an adverse effect on the vertical beam SW and velocity. However, no such effect exists when examining  $u$ ,  $v$ , and the oblique beam SW.

The small median check (Merceret 1997) flags observations which significantly differ from their nearest neighbors. The check, developed using over 20 years of windsonde data at KSC, involves comparing a WS observation at a given time and altitude to the eight observations surrounding it, and the algorithm only performs this check if the WS of interest and at least three neighboring observations exist. First, the check computes the median of the surrounding WS and considers two thresholds:

$$T1 = -0.06z^2 + 1.35z + 3.26, \text{ and} \quad (1)$$

$$T2 = 0.2(WS + WS_{med}). \quad (2)$$

Variables  $z$  and  $WS$  denote the altitude (km) and the WS of interest, respectively, and  $WS_{med}$  represents the median of the surrounding WS. If the difference between  $WS$  and  $WS_{med}$  exceeds the maximum of  $T1$  and  $T2$ , then the check removes data at that range gate. The algorithm performs this check twice to remove any outliers that pass the first check.

MSFC NE uses unique checks to screen convection and the number of FGPs. To address convection, MSFC NE implemented a supervised classification technique (Richards 1993) and training samples of concurrent  $w$  and  $SW$  representing “convective”, “non-convective”, and “possibly convective” environments. These training samples were used to compute the coefficients for the discriminant function

$$DF = K + [w \quad sw_e \quad sw_n \quad sw_v]^* \begin{bmatrix} L_1 \\ L_2 \\ L_3 \\ L_4 \end{bmatrix} + \dots$$

$$[w \quad sw_e \quad sw_n \quad sw_v]^* \begin{bmatrix} Q_{1,1} & Q_{1,2} & Q_{1,3} & Q_{1,4} \\ Q_{2,1} & Q_{2,2} & Q_{2,3} & Q_{2,4} \\ Q_{3,1} & Q_{3,2} & Q_{3,3} & Q_{3,4} \\ Q_{4,1} & Q_{4,2} & Q_{4,3} & Q_{4,4} \end{bmatrix}, \quad (3)$$

where the scalar  $K$  and matrices  $L$  and  $Q$  stand for coefficients corresponding to the covariance of the training samples for each class combination and month. If  $DF$  exceeds zero for the definite versus no convection case,  $DF$  exceeds zero for the definite versus possible convection case, and the posterior probability of convective data existing exceeds 0.95, then the algorithm flags data at the particular gate. Flagged gates are then removed manually if appropriate.

MSFC NE generates a criterion to determine how many FGPs from the oblique beams would yield a root mean square error (RMSE) greater than the acceptable RMSE of the DRWP measurement system. The analysis selects spectra provided by the 50-MHz DRWP operations and maintenance contractor at KSC from three days during 2009: one day during the summer with an afternoon thunderstorm, a dynamic autumn day with moderate winds, and a late-autumn day with strong winds. Using these spectra, MSFC NE simulated the FGP process, and derived the threshold as

$$T = -0.010(FGP_e)^2 - 0.784(FGP_e) + 20.309 - FGP_n \quad (4)$$

In Equation (4),  $FGP_n$  and  $FGP_e$  represent the FGPs from the north and east beams, respectively. If  $T$  falls below zero, then the algorithm removes data at the gate. After performing all automated QC checks for a given day, the algorithm removes data with no surrounding output to enhance the continuity of the database. Barbré (2012) contains a detailed description of the methodology and results of this analysis.

The 915-MHz DRWP automated QC algorithms largely rely on Lambert et al. (2003), and performs several preprocessing steps on all five DRWPs during a selected day. First, the preprocessing algorithm fills data gaps to ensure that no more than 15 minutes exist between each data record. Next, the algorithm removes duplicate profiles with the same DRWP identification. Last, the algorithm determines if the horizontal wind computation includes data from the vertical beam by comparing the number of vertical beam consensus records to the required number of records to generate a consensus. If this check fails at a particular gate, then the algorithm removes the vertical beam’s radial velocity and SNR, but retains the oblique beam’s radial velocity and SNR since this check only pertains to the vertical beam.

Similar to that of the 50-MHz DRWP, the 915-MHz DRWP automated QC process performs several threshold checks in sequence. Table 3 presents each check and its threshold in sequential order. Automated

**Table 3:** Automated QC thresholds for the 915-MHz DRWP QC process. The process removes data that meet the criteria in the threshold column.

QC Check	Threshold
Number of vertical beam consensus records*	less than the number of required consensus records
Consensus averaging period**	< 6 minutes
Number of oblique beam consensus records	less than the number of required consensus records
SNR	< -20 dB
Unrealistic wind	WS < 0 m/s, WD < 0°, or WD > 360°
vertical velocity	w > 10 m/s
convection	see text
RFI	see text
Vector shear	> 0.1 s <sup>-1</sup>
Small median	see text
Isolated datum	see text
* Only data from vertical beam removed	
** Entire profile removed	

QC on the horizontal winds first consists of ensuring a long enough consensus-averaging period exists and that an adequate number of consensus records from the oblique beams exist. Next, the process applies threshold checks for SNR, unrealistic wind, vertical velocity, convection, radio frequency interference (RFI), and vector shear. Last, the process removes data that fail small median and isolated-datum tests. The remainder of this section describes the rationale for each check.

Several automated checks follow a process similar to that in Lambert et al. (2003) with a few very minor modifications. First, the automated QC process applies a consensus-averaging period check to ensure that the horizontal wind computation utilizes radial velocity estimates over at least half of the measurement interval. If this check fails, then the QC process removes the entire profile. Next, the algorithm removes data from range gates containing a number of oblique beam consensus records that fall below the number of records required to generate a consensus. The SNR check applies to all beams that the algorithm uses to compute horizontal winds. If any applicable beam's SNR falls below -20 dB, then the QC process considers the return signal too weak to adequately measure the Doppler shift necessary to compute the radial velocity. After checking for winds that cannot physically occur and for radial velocities that exceed the DRWP's Nyquist velocity, the QC process applies a vertical velocity check to ensure that extreme vertical velocities do not corrupt horizontal wind measurements by violating the triangulation algorithm's homogeneity assumption. This check only affects vertical velocities greater than +10 m/s, and not vertical velocity magnitudes exceeding 10 m/s. Although the manual QC likely removes most cases where  $w$  falls below -10 m/s, one must ensure that a given application does not include these winds, especially for applications involving vertical velocities. After implementing checks on convection and

RFI (discussed below), then the QC process performs a vector shear check following Lambert et al. (2003) and its rationale that shears exceeding 0.1 s<sup>-1</sup> either indicate incorrect data or occur in extreme events which violate the triangulation algorithm's homogeneity assumption.

The QC process applies the convection algorithm from Lambert and Taylor (1998) to flag cases where heavy rain or strong convection could have caused the 915-MHz DRWP to track raindrops instead of air motions or could have violated the triangulation algorithm's homogeneity assumption. As Lambert et al. (2003) states, one can use the 915-MHz DRWP  $w$  and SNR to distinguish convective versus non-convective profiles, as convection and rain tend to produce larger downward motion and enhanced return signal. After converting  $w$  to knots, the algorithm inputs  $w$  and the vertical beam's SNR into

$$L = -1.731 + 0.298(w_{kt}) + 0.014(SNR). \quad (5)$$

In Equation (5),  $w_{kt}$  stands for the vertical beam's radial velocity in knots, which is positive for motions toward the radar, and  $SNR$  denotes the vertical beam's SNR. This check flags and removes data at the given range gate for positive  $L$ . Equation (5) differs from Lambert et al. (2003) in that the second term's coefficient is positive instead of negative. Manual QC removed convective events in the POR before 6 June 2003, analogous to the 50-MHz DRWP QC process, to protect against the check flagging non-convective events. However, the automated algorithm flags appropriate data with few exceptions. For this reason and to enhance efficiency, the automated convection check removed events from 6 June 2003 throughout the rest of the POR. As a result, the archive retains some flagged data that exist before 6 June 2003.

The automated QC includes a check for RFI, which can cause rather obvious signatures in radial velocity and

wind components. RFI generally causes large, unreasonable vertical velocities concurrent with radial velocities from all beams that do not differ much in magnitude. In addition, RFI signatures generally exist over a large vertical extent (1-2 km) within individual profiles, and tend to produce constant wind component profiles which do not coincide with the profile at lower altitudes. The automated QC thus contains a check based on the recommendation in Lambert et al. (2003), and removes the winds at an individual gate if  $w$  exceeds 5.0 m/s and the radial velocity from all beams fall within 0.5 m/s of each other. MSFC NE intentionally uses a more relaxed threshold for  $w$  than what Lambert et al. (2003) recommends (2.0 m/s) because of the unknown effects of implementing the check at the time of development. A manual RFI check also exists using a  $w$  threshold of 2.0 m/s. However, one can discern RFI situations so easily that MSFC NE recommends removing them manually without a  $w$  threshold. Figure 5 shows a before-and-after case where manual QC removes data that RFI likely contaminated.

The small-median check for the 915-MHz DRWP uses the same thresholds as Lambert et al. (2003), but with slightly different input data. The check computes the difference between median of a report's surrounding wind components ( $u_m, v_m$ ) and the observed wind components ( $u_i, v_i$ ) if at least four valid wind reports exist surrounding the wind of interest. The algorithm removes data if either difference exceeds its respective threshold ( $T_u, T_v$ ), which is defined by

$$T_u = \max(T_{u1}, T_2) \text{ and} \quad (6)$$

$$T_v = \max(T_{v1}, T_2), \quad (7)$$

where

$$T_{u1} = 0.2|u_m + u_i|, \quad (8)$$

$$T_{v1} = 0.2|v_m + v_i|, \text{ and} \quad (9)$$

$$T_2 = a(Ah^2 + Bh + C). \quad (10)$$

In  $T_2$ ,  $a = 0.67$  m/s,  $A = -6.127\text{E-}8$  m<sup>-2</sup>,  $B = 0.0012$  m<sup>-1</sup>,  $C = 7.3834$ , and  $h$  stands for altitude (m). If fewer than four wind reports surround the wind in question, then the algorithm does not perform this check. As with the 50-MHz DRWP, the QC process implements this algorithm twice to ensure consistency with nearest neighbors. After performing all automated QC checks for a given day, the algorithm applies an isolated datum check identical to that of the 50-MHz DRWP QC process, removing data with no surrounding valid measurements.

### 3.3 Manual Quality Control Process

MSFC NE manually examines each day's output for temporal and spatial inconsistencies after completing the automated QC process. This manual process applies identically to both the 50- and 915-MHz DRWP archives, except that one must examine up to five 915-MHz DRWP time-height sections of a given variable during each day.

Using the respective GUI, one draws a time-height box to surround regions that contain suspect data, and removes data that fail a specified criterion of the variable in question located within the selected time-height region. Spatial and / or temporal discontinuities of multiple variables within the same time-height region provide greater evidence to remove the data in question. In addition, the manual QC process examines changes in  $u$  and  $v$  at each altitude to detect the edges of radar sidelobes and ground clutter, and logs each check for reference. For the 50-MHz DRWP, the manual QC process flags data separately that are contaminated by convection or ground clutter. The 915-MHz DRWP QC process also contains a separate flag for convection-contaminated data that the process removes manually during the early part of the POR, but does not contain a separate flag to indicate ground clutter.

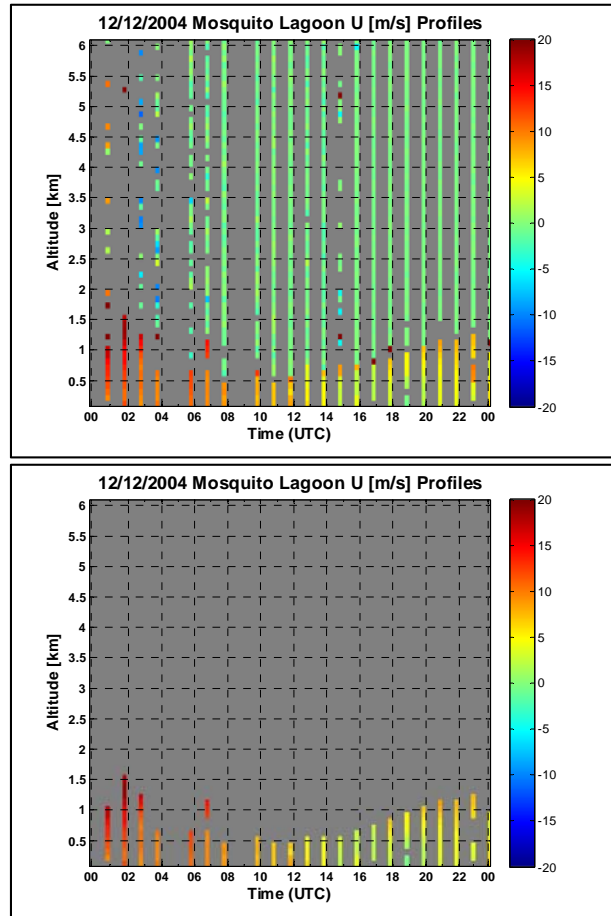


**Figure 5:** Example time-height section of ML  $u$  (m/s) before (top) and after (bottom) implementing the QC process. The x- and y-axes represent time (UTC) and altitude (km), respectively.

One can also compare wind components from LR balloons and the DRWP to determine the quality of DRWP measurements on a given day. DRWP data and available balloon data from the TRMM archive were used to examine the characteristics of the wind components from both sources. Following Shuttle DOL procedures,

this comparison examines wind components from the 50-MHz DRWP wind profile measured roughly 30 minutes after the balloon launch to minimize errors in the comparison from the balloon's rise rate. Similarly, the comparison examines the 915-MHz DRWP wind profile with the timestamp nearest to 10 minutes after the balloon launch because the comparison between these two sources applies at lower altitudes. If the DRWP profile does not compare well with an accepted balloon profile (Figure 6, top panel), then the QC process removes DRWP measurements exhibiting the erroneous trait. Conversely, if the profiles show similar characteristics from both sources (Figure 6, bottom panel), the QC process retains the 50-MHz DRWP winds.

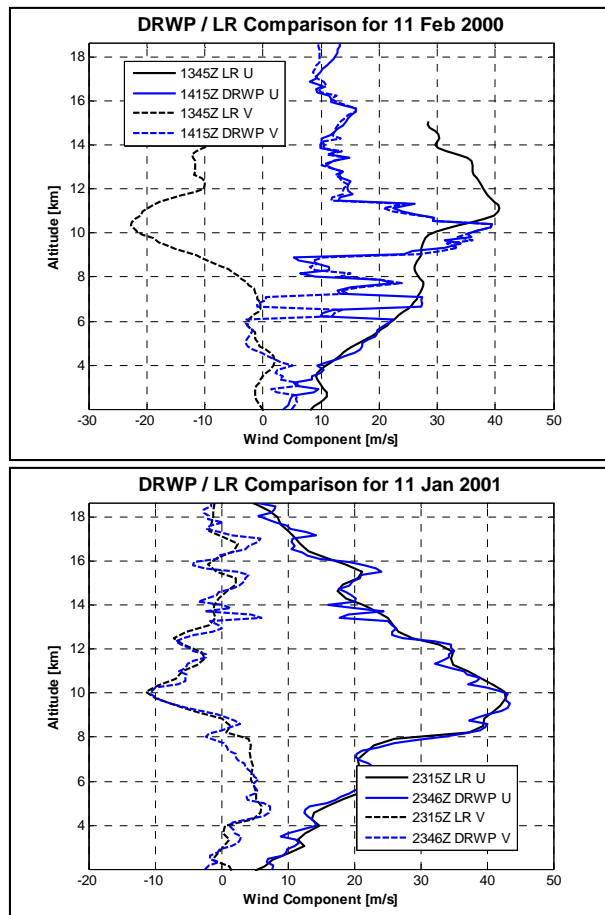


**Figure 6:** Comparisons of  $u$  and  $v$  from the 50-MHz DRWP and a rawinsonde for 11 February 2000 (top) and 11 January 2001 (bottom). The x- and y-axes depict wind components (m/s) and altitude (km), respectively. Blue and black lines denote DRWP and balloon data, respectively; and solid and dashed lines represent the  $u$  and  $v$  components, respectively.

## 4. QUALITY CONTROL RESULTS

### 4.1 50-MHz DRWP

Table 4 presents the number and percentage of gates affected by each 50-MHz DRWP QC check. The QC process assigns a flag to each check, and records the number of times an individual flag occurs in each month. Note that this table differs slightly from Barbré (2012) due to MSFC NE reexamining several days after generating these documents. The entire POR contains 162.1 million gates, with a given month containing 12.2–14.4 million gates. The paper herein notes percentages of affected data as %POR (the percent lowest month to the percent highest month). Missing data account for 35.4% (30.0–41.0%) of all the possible data. The algorithm tallies the missing data flag most often because the flag tends to exist throughout an entire profile, and the flag exists at every gate and timestamp during days in which no data exist. The other checks combined remove an additional 6.4% (3.1–10.5%) of the possible data, with manual QC removing 4.8% (1.8–8.6%) of the data. The convection check removes 0.6% (0.1–1.1%) of the available data. Note that the automated convection algorithm flags 2.6% of the data for the POR, but the convection check only removes 0.6% of the data; indicating the significance of removing flagged data manually. The other automated checks remove no more than 1.0% of the available data for a given month. No observations exist that have unrealistic reports of WS or WD, and the QC'd database contains 58.2% (51.6–64.5%) of the possible wind observations. The 50-MHz DRWP QC process retains 90.1% (84.9–95.0%) of all recorded data.

### 4.2 915-MHz DRWP

Table 5 depicts the number and percentage of gates affected by each check in the 915-MHz DRWP QC process for each month across all five 915-MHz DRWPs. The entire POR contains 91.5 million gates from all five DRWPs, with a given month containing 6.8–8.4 million gates. Missing data account for 74.1% (67.1–80.4%) of all the possible data. Because the 915-MHz DRWP profiles typically reach 2.0–3.0 km in clear air, missing data exist throughout the top portion of a significant number of 915-MHz DRWP profiles. The other checks combined remove an additional 2.8% (2.2–3.4%) of the possible data. As with the 50-MHz DRWP QC, the manual check dominates the other QC processes by removing 1.4% (1.0–1.6%) of the data. The convection check removes 0.7% (0.3–1.4%) of the data, and the other automated checks remove no more than 1.0% of the possible data during a given month. Five checks affect at most 0.1% of the data during each month, but only the unrealistic wind check does not flag any data. The 915-MHz DRWP QC process retains 89.9% (83.7–91.1%) of all recorded data.

**Table 4:** Number (top) and percentage (bottom) of range gates that the 50-MHz DRWP QC process affects. Data for each month exists on each row and data for each QC process exists on each column. The process does not remove data matching the criteria in the first three columns. Percentages are rounded to the nearest tenth of a percent.

	No Flag	Vert QC	Conv Flag	Missing	Unreal	SW	DRWP Shr	Vert Spd	FGP	MET Shr	Median	Clutter	No Signal	Isolated	Manual	Conv	Removed	Retained	Total
Jan	7316020	60888	243135	5163528	0	10253	20120	1064	73110	58	1356	30028	4728	189	329022	19158	5652614	7620043	13272657
Feb	7423884	58632	390218	3668893	0	10253	24042	1596	76885	56	1109	36433	4445	178	508960	43140	4375990	7872734	12248724
Mar	8251799	65234	273503	4274180	0	13995	20830	2167	52208	60	1382	28716	5657	236	289434	39018	4727883	8590536	13318419
Apr	7704625	59608	213625	3951625	0	15614	25165	1761	108530	64	1372	23089	13918	838	761762	76682	4980420	7977858	12958278
May	7337796	95248	467660	4380353	0	5804	14832	3576	100244	23	929	25675	5898	226	720776	130001	5388337	7900704	13289041
Jun	7182674	131101	252861	3920058	0	17129	18983	5170	41367	28	1639	14872	3159	271	1100205	146821	5269702	7566636	12836338
Jul	7046816	193571	131636	5096108	0	14354	18488	3131	46424	12	2279	11502	5229	306	637935	127114	5962882	7372023	13334905
Aug	6882160	207671	209339	5790597	0	12166	17579	3121	46315	7	902	13656	5441	317	861692	105957	6857750	7299170	14156920
Sep	7423711	212965	556514	4385174	0	8803	27689	4252	142618	40	1385	12330	11644	371	1037865	143930	5776101	8193190	13969291
Oct	7514680	160926	339670	5491363	0	14680	30086	4685	55093	48	1341	9870	4597	171	678566	77279	6367779	8015276	14383055
Nov	7072924	121311	692872	5372878	0	14880	27970	1661	99956	89	1921	9831	16592	1001	516016	43524	6106319	7887107	13993426
Dec	7436786	91241	489712	5889984	0	8819	19376	1098	85635	85	1417	16769	9065	653	261662	36806	6331369	8017739	14349108
Total	88593875	1458396	4260745	57384741	0	146750	265160	33282	928385	570	17032	232771	90373	4757	7703895	989430	67797146	94313016	162110162

	No Flag	Vert QC	Conv Flag	Missing	Unreal	SW	DRWP Shr	Vert Spd	FGP	MET Shr	Median	Clutter	No Signal	Isolated	Manual	Conv	Removed	Retained
Jan	55.1	0.5	1.8	38.9	0.0	0.1	0.2	0.0	0.6	0.0	0.0	0.2	0.0	0.0	2.5	0.1	42.6	57.4
Feb	60.6	0.5	3.2	30.0	0.0	0.1	0.2	0.0	0.6	0.0	0.0	0.3	0.0	0.0	4.2	0.4	35.7	64.3
Mar	62.0	0.5	2.1	32.1	0.0	0.1	0.2	0.0	0.4	0.0	0.0	0.2	0.0	0.0	2.2	0.3	35.5	64.5
Apr	59.5	0.5	1.6	30.5	0.0	0.1	0.2	0.0	0.8	0.0	0.0	0.2	0.1	0.0	5.9	0.6	38.4	61.6
May	55.2	0.7	3.5	33.0	0.0	0.0	0.1	0.0	0.8	0.0	0.0	0.2	0.0	0.0	5.4	1.0	40.5	59.5
Jun	56.0	1.0	2.0	30.5	0.0	0.1	0.1	0.0	0.3	0.0	0.0	0.1	0.0	0.0	8.6	1.1	41.1	58.9
Jul	52.8	1.5	1.0	38.2	0.0	0.1	0.1	0.0	0.3	0.0	0.0	0.1	0.0	0.0	4.8	1.0	44.7	55.3
Aug	48.6	1.5	1.5	40.9	0.0	0.1	0.1	0.0	0.3	0.0	0.0	0.1	0.0	0.0	6.1	0.7	48.4	51.6
Sep	53.1	1.5	4.0	31.4	0.0	0.1	0.2	0.0	1.0	0.0	0.0	0.1	0.1	0.0	7.4	1.0	41.3	58.7
Oct	52.2	1.1	2.4	38.2	0.0	0.1	0.2	0.0	0.4	0.0	0.0	0.1	0.0	0.0	4.7	0.5	44.3	55.7
Nov	50.5	0.9	5.0	38.4	0.0	0.1	0.2	0.0	0.7	0.0	0.0	0.1	0.1	0.0	3.7	0.3	43.6	56.4
Dec	51.8	0.6	3.4	41.0	0.0	0.1	0.1	0.0	0.6	0.0	0.0	0.1	0.1	0.0	1.8	0.3	44.1	55.9
Total	54.7	0.9	2.6	35.4	0.0	0.1	0.2	0.0	0.6	0.0	0.0	0.1	0.1	0.0	4.8	0.6	41.8	58.2

**Table 5:** Number (top) and percentage (bottom) of range gates that the 915-MHz DRWP QC process affects. Data for each month exists on each row and data for each QC process exists on each column. The process does not remove data matching the criteria in the first three columns. Percentages are rounded to the nearest tenth of a percent.

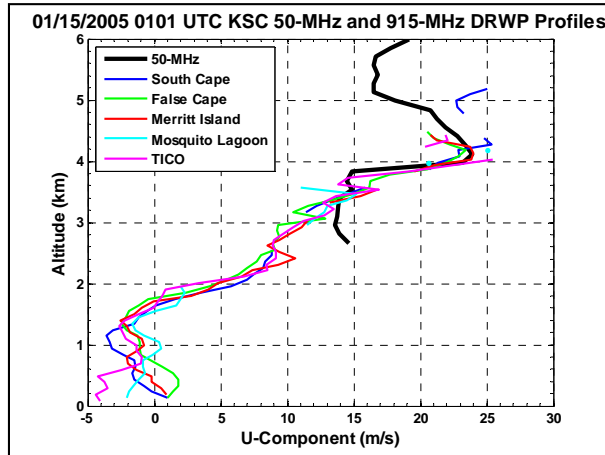
No Flag	Vert QC	Convection Flag	Missing	Consensus Avg. Period	Consensus Records	SNR	Unreal	Vert. Spd	Automated RFI	Met. Shear	Small Median	Isolated Datum	Convection	Manual RFI	Manual	Removed	Retained	Total
1024110	121932	595	5603432	267	8	2388	0	0	39017	10661	4711	18241	34613	163	112701	5826202	1146637	6972839
1085535	108368	173	5392091	483	2	2071	0	0	7117	7548	4397	15156	35527	16	105331	5569739	1194076	6763815
1353323	124915	173	5708068	780	1	2517	0	76	41851	6133	3858	13420	24322	597	70361	5871984	1478411	7350395
1362821	130547	274	5530289	631	1	4059	0	10	49134	7154	4528	16879	23157	6993	83500	5726335	1493642	7219977
1597198	160694	246	6145109	803	0	5538	0	0	11892	5315	5241	14530	52995	516	86876	6328815	1758138	8086953
2061157	220430	337	5178650	758	1	3613	0	2	1894	6404	7532	15421	104495	79	121233	5440082	2281924	7722006
2002964	224682	5	5753530	1000	15	5940	0	0	1379	4833	7499	16791	96876	108	114957	6002928	2227651	8230579
2056467	248852	5	5694674	599	14	8860	0	0	409	4880	6933	16464	88250	54	99443	5920580	2305324	8225904
1828052	200057	58	5354897	472	2	4404	0	0	1876	5510	8581	16935	86685	36	123521	5602919	2028167	7631086
1814913	178985	147	6126155	507	0	4752	0	2	15441	9159	8891	21211	56763	60	133831	6376772	1994045	8370817
1529585	161720	131	5757063	172	0	2027	0	0	19719	10217	5449	18263	30017	10	92304	5935241	1691436	7626677
1371090	145284	158	5524472	407	2548	1543	0	1	32876	9125	4484	17022	40476	446	100605	5734005	1516532	7250537
19087215	2026466	2302	67768430	6879	2592	47712	0	91	222605	86939	72104	200333	674176	9078	1244663	70335602	21115983	91451585

No Flag	Vert QC	Convection Flag	Missing	Consensus Avg. Period	Consensus Records	SNR	Unreal	Vert. Spd	Automated RFI	Met. Shear	Small Median	Isolated Datum	Convection	Manual RFI	Manual	Removed	Retained
14.7	1.7	0.0	80.4	0.0	0.0	0.0	0.0	0.0	0.6	0.2	0.1	0.3	0.5	0.0	1.6	83.6	16.4
16.0	1.6	0.0	79.7	0.0	0.0	0.0	0.0	0.0	0.1	0.1	0.1	0.2	0.5	0.0	1.6	82.3	17.7
18.4	1.7	0.0	77.7	0.0	0.0	0.0	0.0	0.0	0.6	0.1	0.1	0.2	0.3	0.0	1.0	79.9	20.1
18.9	1.8	0.0	76.6	0.0	0.0	0.1	0.0	0.0	0.7	0.1	0.1	0.2	0.3	0.1	1.2	79.3	20.7
19.8	2.0	0.0	76.0	0.0	0.0	0.1	0.0	0.0	0.1	0.1	0.1	0.2	0.7	0.0	1.1	78.3	21.7
26.7	2.9	0.0	67.1	0.0	0.0	0.0	0.0	0.0	0.0	0.1	0.1	0.2	1.4	0.0	1.6	70.4	29.6
24.3	2.7	0.0	69.9	0.0	0.0	0.1	0.0	0.0	0.0	0.1	0.1	0.2	1.2	0.0	1.4	72.9	27.1
25.0	3.0	0.0	69.2	0.0	0.0	0.1	0.0	0.0	0.0	0.1	0.1	0.2	1.1	0.0	1.2	72.0	28.0
24.0	2.6	0.0	70.2	0.0	0.0	0.1	0.0	0.0	0.0	0.1	0.1	0.2	1.1	0.0	1.6	73.4	26.6
21.7	2.1	0.0	73.2	0.0	0.0	0.1	0.0	0.0	0.2	0.1	0.1	0.3	0.7	0.0	1.6	76.2	23.8
20.1	2.1	0.0	75.5	0.0	0.0	0.0	0.0	0.0	0.3	0.1	0.1	0.2	0.4	0.0	1.2	77.8	22.2
18.9	2.0	0.0	76.2	0.0	0.0	0.0	0.0	0.0	0.5	0.1	0.1	0.2	0.6	0.0	1.4	79.1	20.9
20.9	2.2	0.0	74.1	0.0	0.0	0.1	0.0	0.0	0.2	0.1	0.1	0.2	0.7	0.0	1.4	76.9	23.1

## 5. WIND PROFILE SPLICING TECHNIQUE

MSFC NE develops an algorithm that combines concurrent, QC'ed, 50- and 915-MHz DRWP measurements to produce vertically complete profiles. The QC process that the paper has described produces two databases with an overlapping POR from April 2000 through December 2009. One database consists of a single profile at each timestamp reported from roughly 2.5-18.6 km, and another database consists of up to five profiles at each timestamp reported from approximately 0.2-3.0 km (Figure 7). MSFC NE generates the algorithm to effectively splice concurrent measurements while preserving the characteristics of the wind environment within the transition region, which is typically around 2.0-4.0 km. Within the transition region, measurements from both DRWP sources exist at the same altitude, or a gap exists between the top of the input 915-MHz DRWP profile and the bottom of the input 50-MHz DRWP profile. The general algorithm consists of either faring or interpolating (i.e., "splicing") the 915-MHz DRWP profile into the 50-MHz DRWP profile in the transition region, then filtering the spliced profile so that the 915-MHz DRWP's contribution to the spliced profile does not contain spectral energy at wavelengths too small for the 50-MHz DRWP to measure. The algorithm then generates a single composite boundary layer profile, which represents the boundary-layer wind environment at a given timestamp. This section describes in detail the methods MSFC NE uses to generate the database of vertically complete DRWP profiles.



**Figure 7:** QC'ed 50- and 915-MHz DRWP  $u$  (m/s) profiles versus altitude (km). The black line represents the 50-MHz DRWP  $u$ , and other colors show  $u$  from concurrent 915-MHz DRWP measurements.

### 5.1 Preprocessing

Because each DRWP systems reports at different temporal and spatial intervals, as well as across different altitude ranges (see Table 1), one must obtain two concurrent profiles with data reported at the same altitudes before performing any splicing. After finding an individual 915-MHz DRWP profile that contains the

timestamp closest to the 50-MHz DRWP timestamp, the algorithm fills gaps in each profile and interpolates each profile's wind components to a 50-m interval at altitudes ranging from 100-18,600 m. This operation generates two separate 371-element vectors. One vector contains data at all the altitudes applying to the 915-MHz DRWP profile and the other vector contains data at all the altitudes applying to the 50-MHz DRWP profile, with both profiles containing data within their respective altitude ranges. The algorithm fills gaps by interpolating wind components to a 50-m interval within the gaps, and flags gaps exceeding six consecutive data points (300-m interval) and 10 consecutive data points (500-m interval) from the input 50- and 915-MHz DRWP profiles, respectively. Barbré (2013) contains analyses that support the selection of the 50-m altitude interval and the gap size criteria.

### 5.2 Algorithm Development

The DRWP splicing algorithm primarily consists of procedures to splice each interpolated, concurrent 50- and 915-MHz DRWP profile in the transition region. MSFC NE develops this algorithm using several test cases, and the report uses a few of these test cases to communicate the algorithm's main attributes. One finds an ideal situation and intentionally manipulates different profiles to generate a specific test case, and Barbré (2013) contains all test cases for reference. The algorithm examines each 915-MHz DRWP profile independently with the concurrent 50-MHz DRWP profile – ignoring any contribution from other 915-MHz DRWPs. If only one DRWP system contains data at a given altitude, then the spliced profile only contains data from that system. If the 915-MHz DRWP profile overlaps the 50-MHz DRWP profile, then the algorithm averages the weighted wind components at altitudes that contain data from both DRWP sources. This technique utilizes a Gaussian weighting scheme that emphasizes the 915-MHz DRWP at the bottom of the transition region and accentuates the 50-MHz DRWP at the top of the transition region. MSFC NE uses the weights in this manner to help protect against ground clutter effects from the 50-MHz DRWP profile near the bottom of the transition region and effects from weak signal from the 915-MHz DRWP at the top of the transition region. As Figure 8 illustrates, the weight consists of a value ranging from zero to one as altitude within the transition region increases. Thus, the weight defines the 50-MHz DRWP profile's contribution to the spliced profile. The algorithm then computes the spliced DRWP's wind component as

$$U(z) = W(z) * U_{50}(z) + [1 - W(z)] * U_{915}(z) \quad (11)$$

where  $U$ ,  $W$ ,  $U_{50}$ , and  $U_{915}$  represent the computed wind component, weight, input 50-MHz DRWP wind component, and input 915-MHz DRWP wind component, respectively, at altitude  $z$ . In the example provided in Figure 8, the transition region extends from 2.7-4.4 km. In this case,  $W$  starts at 0.0 below 2.7 km, transitions from 0.0-1.0 from 2.7-4.4 km, and is 1.0 above 4.4 km.

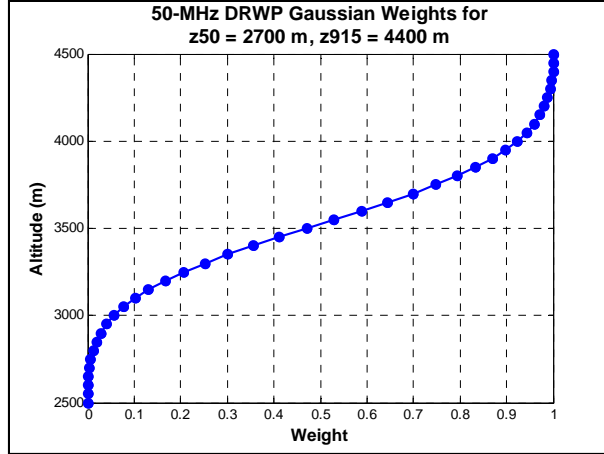


**Figure 8:** Weights used to compute the spliced DRWP's wind components for the overlapping altitude region extending from 2.7-4.4 km. The x- and y-axes denote the weight (dimensionless) and altitude (m), respectively.

Applying Equation (11) with the appropriate  $W$  at each  $z$  thus produces the spliced profile, which merges the 915-MHz DRWP winds into the 50-MHz DRWP winds within the transition region. Figure 9 also presents the spliced profile for this individual case. Note that  $W$  at a given altitude depends strongly on the extent of the overlapping region. If the 915-MHz DRWP profile does not overlap the 50-MHz DRWP profile, then the algorithm linearly interpolates each wind component through the altitude region containing missing data using the highest 915-MHz DRWP wind and the lowest 50-MHz DRWP wind as endpoints. After splicing the profiles, the algorithm removes excessively large gaps using the criteria that the preprocessing section presents and interpolates through any winds that exceed a  $0.1 \text{ s}^{-1}$  vector shear over 50-m in order to remove discontinuities that the splicing process may have generated.

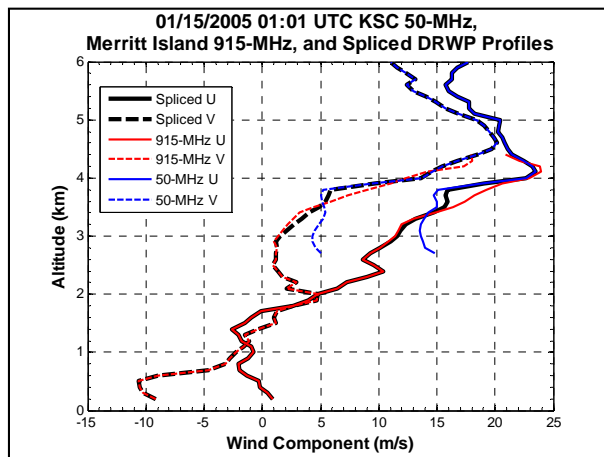


**Figure 9:** Example wind component (m/s) profile versus altitude (km). Solid and dashed lines represent  $u$  and  $v$ , respectively. Red, blue, and black lines stand for the concurrent 915-MHz, 50-MHz, and spliced DRWP profile, respectively.

The algorithm then smoothes the profile's wind components within the lower part of the transition region to help protect against remaining unrealistically large shears. The splicing algorithm works well when differences of only a few m/s exist between the winds at the top of the input 915-MHz DRWP profile and the winds at the bottom of the input 50-MHz DRWP profile. However, one can and should expect to encounter cases where the top of the 915-MHz DRWP profile does not represent the bottom of the 50-MHz DRWP profile for both meteorological and non-meteorological reasons. In addition, the spliced profile becomes very sensitive to the winds at the bottom of the 50-MHz DRWP and the top of the 915-MHz DRWP in cases where little or no overlap exists. Therefore, the splicing process could compute erroneous winds within the transition region in these cases. First, the algorithm removes data from the original spliced profile at altitudes 1.0 km above the lowest altitude that contains data from inputs other than 915-MHz DRWP measurements. Next, the algorithm linearly interpolates the wind components between the gap's endpoints. Last, the algorithm computes the weighted average of each wind component using

$$U(z) = W(z) * U_{int}(z) + [1 - W(z)] * U_{orig}(z), \quad (12)$$

where  $U_{out}$ ,  $U_{int}$ , and  $U_{orig}$  represent the resulting wind component, interpolated wind component, and original wind component, respectively, at altitude  $z$ . Weight  $W$  ranges from 0.0-1.0 in a Gaussian manner, where  $z$  designates the altitudes within the lowest 1.0 km of the transition region. Implementing Equation (12) generates profiles that transition more gradually from the top of the 915-MHz DRWP profile into the bottom of the 50-MHz DRWP profile.

The DRWP splicing algorithm's final step consists of filtering the profile to a constant cutoff wavelength and performing a second shear check. Although the spliced profile contains data spaced at a constant altitude interval of 50 m, the spectral characteristics of the profile can differ as a function of altitude region. Specifically, the lower part of the profile from the 915-MHz DRWP is Nyquist-limited at roughly 200 m wavelength; while the upper part of the profile from 50-MHz DRWP is Nyquist-limited at about 300 m wavelength. Also, the profile in the transition region could contain some small, fictitious features from implementing the splicing algorithm. Thus, MSFC NE applies a six-pole Butterworth filter (<http://www.mathworks.com/help/signal/ref/butter.html>) to attenuate features from each wind components' profile that do not exceed 300-m wavelength with 95% gain at 300 m. Thus, the filtered profile does not contain features in one part of the profile that both DRWP sources cannot resolve. Finally, the splicing algorithm removes data that fail a second shear check and flags the profile. Flags exist in the spliced DRWP database that indicate how the splicing algorithm generates the winds at each time and altitude.

### 5.3 Generating a Composite Boundary Layer Profile

MSFC NE develops a process to generate a single profile representing the wind environment at each timestamp. Implementing the DRWP splicing algorithm produces up to five simultaneous profiles, with each profile differing – potentially significantly – in the atmospheric boundary layer. There can exist up to five simultaneous spliced profiles, but having five spliced profiles is not required. Because only one 50-MHz DRWP measurement exists at a given time, each of the simultaneous spliced profiles do not differ above the highest altitude of the transition regions. Figure 10 illustrates this concept, where the spliced profiles from each 915-MHz DRWP source differ below roughly 3.3 km. In addition, discontinuities in one or more profiles may exist in this altitude region. For example, one  $v$  profile contains a spike at 1.8 km while all the other profiles contain a consistent  $v$  profile in the same altitude region. In order to provide end users with the capability to select one profile to represent the entire altitude region (0.2-18.5 km), and to generate a larger sample of wind profiles using multiple 915-MHz DRWPs, MSFC NE generates a “composite” spliced profile using all available spliced profiles at a given timestamp. This composite profile essentially consists of a consensus-averaged profile within and below the transition region and the 50-MHz DRWP profile above the transition region. Regarding terminology, the paper herein refers to the spliced profiles generated from a given 915-MHz DRWP by name, and refers to the composite profile as the consensus of all the spliced profiles using the 50-MHz DRWP and the available 915-MHz DRWP measurements.

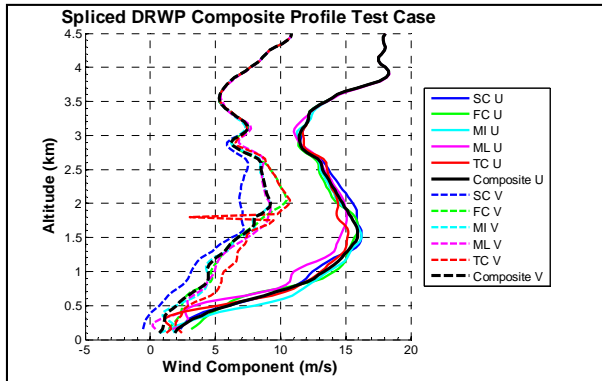


**Figure 10:** Hypothetical test case of simultaneous spliced wind component (m/s) profiles from each of the five 915-MHz DRWP measurements and the concurrent 50-MHz DRWP measurement versus altitude up to 6 km. Each non-black line shows the spliced profile using the respective 915-MHz DRWP, and the black line represents the composite profile. Solid and dashed lines depict  $u$  and  $v$ , respectively.

MSFC NE first categorizes the five 915-MHz DRWPs as “dominant” or “recessive” to appropriately tailor the algorithm to applications that could utilize the composite profile. The algorithm to produce a composite profile

weights the winds from the SC, FC, and MI profiles more heavily than the winds from the ML and TC profiles. Proximity to the coast and the 50-MHz DRWP, as well as subjective evaluation during the 915-MHz DRWP QC process, determined the grouping of the 915-MHz DRWPs in this manner.

MSFC NE designs this algorithm to generate the best composite boundary layer profile from the available spliced profiles, as Figure 10 highlights by not including the spike from the TC profile. The algorithm implements the following process on each altitude individually starting at the bottom of the profile, and ignores any profiles that do not reach 500 m below the lowest altitude containing data from which the splicing algorithm uses only the 50-MHz DRWP. First, the algorithm to generate a composite profile computes a reference wind as

$$U_{ref} = \frac{U_{SC} + U_{FC} + U_{MI}}{N_1} \text{ and } V_{ref} = \frac{V_{SC} + V_{FC} + V_{MI}}{N_1}, \quad (13a)$$

where  $N_1$  stands for the number of valid wind reports from the SC, FC, and MI DRWPs. Thus,  $N_1$  ranges from 1-3 if data from SC, FC, or MI exist. If no data from SC, FC, nor MI profiles exist, then the algorithm computes the reference wind as

$$U_{ref} = \frac{U_{ML} + U_{TC}}{N_2} \text{ and } V_{ref} = \frac{V_{ML} + V_{TC}}{N_2}, \quad (13b)$$

where  $N_2$  stands for the number of valid wind reports from the ML and TC DRWPs, thus ranging from 1-2. In Equation (13),  $U_{ref}$  and  $V_{ref}$  represent the reference wind components, and the wind components' subscripts denote the spliced profile that the algorithm uses. Note that the algorithm only uses the ML and TC profiles to compute the reference wind if neither the FC, SC, nor MI profile exist. Next, the algorithm calculates residuals from the reference wind as

$$R = \sqrt{(U_{ALL} - U_{ref})^2 + (V_{ALL} - V_{ref})^2} \quad (14)$$

where vectors  $U_{ALL}$  and  $V_{ALL}$  represent the wind components from each of the available spliced profiles at the given altitude. Therefore, vector  $R$  contains the vector differences between the reference wind and the wind from each of the (up to) five input profiles. Then, the algorithm generates weights for each input profile as a function of  $R$ :

$$W = \frac{(1/R)}{\sum (1/R)}. \quad (15)$$

In Equation (15), vector  $W$  represents the weight assigned to each of the input profiles, and depends on two characteristics of the spliced profiles at the given timestamp. First, the relative difference between the input wind and the reference wind influence  $W$ , with a larger  $W$  corresponding to a smaller  $R$  and vice versa. Second, the number of available spliced profiles contributes to  $W$  from an individual profile. The quantity  $W$  always sums to one and quantifies how much an individual profile's wind

contributes to the composite wind. Note that  $W$  behaves as a function of  $1/R$ , which implies that  $R$  cannot equal exactly 0.000 m/s. To avoid this result, the algorithm rounds  $R$  to the nearest hundredth and replaces instances where  $R = 0.000$  m/s with  $R = 0.001$  m/s before applying Equation (15). This operation not only eliminates a possible divide-by-zero error, but also ensures that instances where  $R$  equals exactly 0.000 m/s (before manipulation) contain the largest weight. The algorithm computes the composite wind components as

$$U_c = \sum(W * U_{ALL}) \text{ and } V_c = \sum(W * V_{ALL}), \quad (16)$$

where  $U_c$  and  $V_c$  stand for the composite wind components at the given altitude. The algorithm then checks for excessive shear before applying the aforementioned process at the next altitude. If the 50-m vector shear at the altitude of interest exceeds  $0.1 \text{ s}^{-1}$ , then the algorithm removes the wind with the highest weight and repeats the process to protect against gross discontinuities in the profile. Also to maintain vertical consistency, the algorithm averages  $U_{ref}$  and  $V_{ref}$  from Equation (13) with the previous altitude's  $U_c$  and  $V_c$  before implementing Equation (14). After performing this process at all altitudes, the algorithm applies a 300-m low pass Butterworth filter to the composite profile. Barbré (2013) provides an analysis which reveals that implementing this process maintains the spectral content of the input profiles at wavelengths that the DRWP can measure.

Generating a composite profile helps eliminate outliers and utilize the most representative data available. The following list contains some attributes of the composite profiles:

- No composite wind exists where no input winds exist, and a composite wind exists where at least one input wind exists.
- The algorithm does not contain an interpolation scheme nor does it attempt to fill gaps.
- No difference exists between the composite wind and an individual input wind if only one input wind exists – regardless of the input wind's source.
- No difference exists between the composite profile and a profile from a dominant source if only one dominant source contains data.
- The algorithm weights input profiles differently in altitude regions where profiles from all sources do not exist, and weights input winds independent of altitude.
- The algorithm weights the composite profile toward the mean of the dominant profiles, which helps mitigate including any discontinuities in individual input profiles. However, the composite profile contains discontinuities if they exist in input profiles from dominant sources and the discontinuities pass the shear check.

## 6. VALIDATION ANALYSES

MSFC NE utilizes wind shear and wind change analyses to check the QC and splicing processes. These

analyses examine all profiles that contain continuous data from 0.25-6.10 km and MSFC NE regenerates the database if these analyses produce anomalies. MSFC NE performs numerous analyses and generates a significant number of plots. Thus, this paper discusses results from representative cases.

The wind shear analysis consists of plotting selected percentiles and the maximum of the 50-m vector shear at each altitude, and examines the entire POR at once. Figure 11 shows the results for the composite profiles. Discontinuities in the shear profiles at a selected percentile exist around 0.2 km, 2.0-4.0 km, and 18.6 km. Near 0.2 km, wind shears significantly exceed shears that exist immediately above this layer. The archive retains these shears because surface layer effects, such as thermal inversions, could cause large vertical gradients in WS and / or WD at very low altitudes. Thus, one cannot uniquely attribute these shears to suspect data. The shear profiles' behavior from roughly 2.0-4.0 km results from implementing the DRWP splicing algorithm within the transition region, so one should expect some discontinuity in wind shears within this altitude region. The anomaly at the top of the profile raises some concern, as no meteorological explanation exists to merit shears at 18.6 km significantly exceeding shears which exist immediately below that altitude and the splicing algorithm does not manipulate data within this altitude region. In addition, MSFC NE uses the DRWP wind at the highest reporting altitude to initialize Earth-Global Reference Atmospheric Model (Earth-GRAM, Leslie and Justus 2010) profiles for SLS. Thus, the spliced DRWP archive contains data up to 18.45 km to avoid the potential use of suspect winds to set Earth-GRAM's initial conditions – where any errors in the wind at the initial altitude could propagate to higher altitudes.

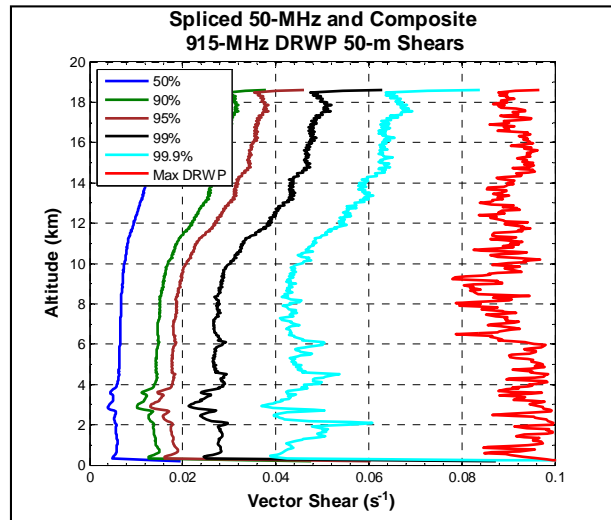


**Figure 11:** Composite profiles' vector shear ( $\text{s}^{-1}$ ) across a 50-m interval at selected percentiles versus altitude (km).

Similar to the aforementioned shear analysis, the first of two wind change analyses consists of examining the vector wind change at selected percentiles and the

maximum vector wind change at each altitude. Figures 12 and 13 present an example case. In Figure 12, January's maximum 2.0-hour wind change near 0.5 km of roughly 32 m/s exceeds the maximum wind change at all other altitudes. Figure 13 presents  $v$  during the day of the wind change in question. In this case, the wind change is validated as  $v$  changes from roughly 15 m/s to approximately -5 m/s from 0630-0830 UTC due to a valid meteorological event. This analysis entails examining numerous events such as these, and regenerating the database if necessary. Preliminary wind change analyses revealed that ground clutter, which is very difficult to completely eliminate during QC, could have contaminated data at the lowest 915-MHz DRWP range gate. Thus, the algorithm removes data from the first range gate (either at 87 m or 130 m) before implementing the DRWP splicing procedure. Thus, the spliced DRWP archive does not contain data below 200 m, and many profiles do not contain data below 250 m.

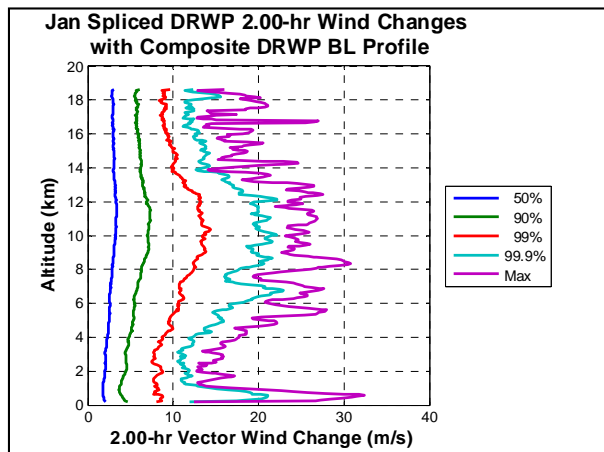


**Figure 12:** Composite profiles' 2.0-hr vector wind change (m/s) at selected percentiles versus altitude (km) during January.

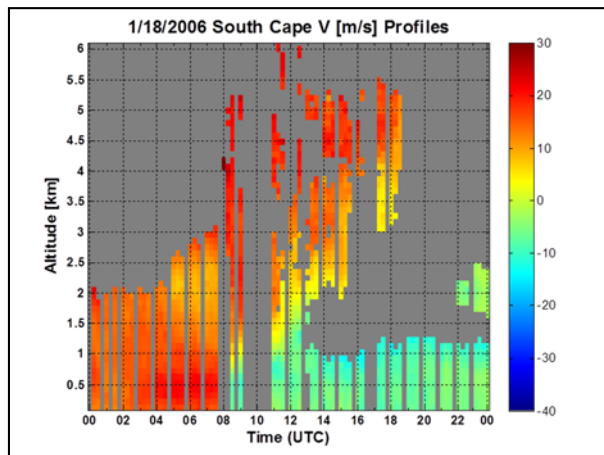


**Figure 13:** Time-height section of  $v$  (m/s) from the SC DRWP during 18 January 2006. The x- and y-axes represent time (UTC) and altitude (km), respectively.

The second wind change analysis examines the distribution of the maximum wind component change in each profile over a given time interval. Figure 14 shows the distributions of maximum wind component change magnitudes over 1.5- and 2.0 hours. One should expect that larger wind changes occur over longer time intervals, which implies that the 2.0-hour wind changes should envelope the 1.5-hour wind changes. However, the maximum 1.5-hour change of roughly 38 m/s exceeds the maximum 2.0-hour change of near 33 m/s. Examination of the event containing the large 1.5 hour wind change shows that from roughly 1400-1600 UTC on 29 November 2009 (Figure 15),  $v$  changed from near 15 m/s to around -20 m/s from roughly 8.0-10.0 km. Thus, the archive retains the wind profiles that produce the maximum 1.5-hour wind changes.

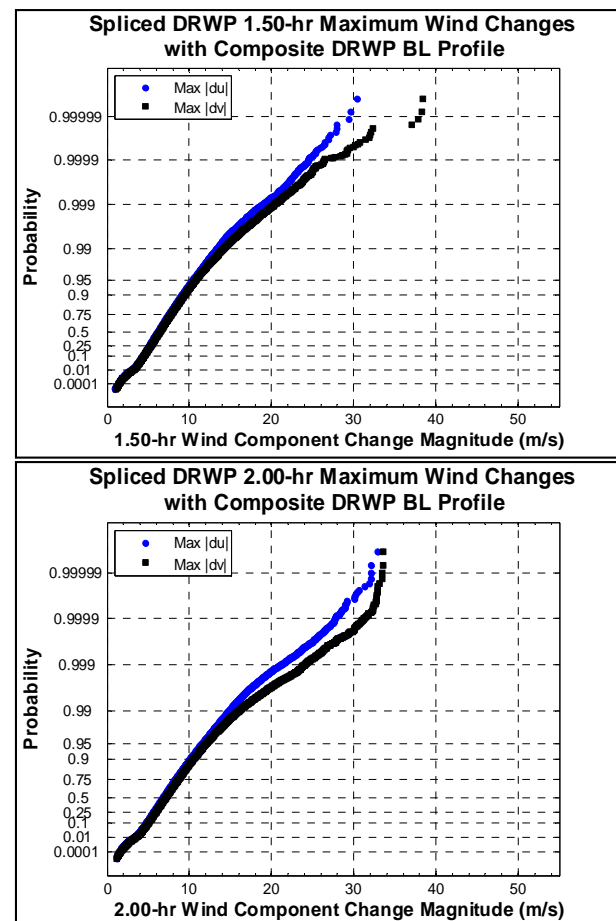


**Figure 14:** Cumulative probability distributions of maximum wind component change magnitude over 1.50 hours (top) and 2.00 hours (bottom). Blue and black points represent the change in  $u$  and  $v$ , respectively.

## 7. SAMPLE SIZE AND SUBSETS

The spliced DRWP archive contains several thousand complete profiles that one can use to characterize the wind environment near KSC from 0.25-18.45 km. Figure 16 presents the number of profiles in the archive that contain data at all altitudes from 0.25-18.45 km

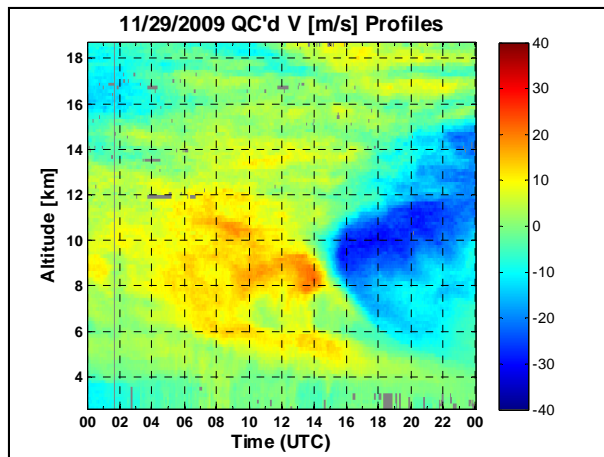


**Figure 15:** Time-height section of  $v$  (m/s) from the 50-MHz DRWP during 29 November 2009. The x- and y-axes depict time (UTC) and altitude (km), respectively.

during each month from each of the six possible profile sources. During an individual month, roughly 23,000-32,000 complete profiles exist from the composite profiles' archive, and anywhere from approximately 5,000-27,000 complete profiles exist from an archive utilizing an individual 915-MHz DRWP. Significantly fewer ML profiles exist because the 915-MHz DRWP QC process removes suspect winds at low altitudes from many of the profiles. Generally, the SC and MI archives contain the largest sample of profiles using an individual 915-MHz DRWP during a given month. The composite profiles' archive contains the most data during an individual month because not all data from a single 915-MHz DRWP must exist to generate a complete composite profile if other 915-MHz DRWPs contain concurrent data at the appropriate altitudes. The plot also reveals that, in general, less data exist during the cool season than the warm season. This attribute likely results from the drier cool-season climate causing more frequent occurrences where the 915-MHz DRWP produces a profile that does not reach a sufficient altitude to generate a spliced profile (Murri 2011). Adjusting the altitude requirements would increase the number of available profiles.

MSFC NE maintains the spliced DRWP archive, and has developed subsets from this archive for specific analyses and to address flight vehicle requirements. The files containing the spliced data and associated flags contain numerous profiles that may not suffice for a given application due to either insufficient altitude coverage and/or missing data gaps. Subsets thus provide end users with the necessary data without having to carefully select criteria for extracting valid profiles. One should note that multiple applications can use the same subset. MSFC NE generates several subsets for space vehicle programs that need to incorporate wind profiles from near the surface to 18.5 km in vehicle analyses:

- 4,000 seasonal one-hour triplets for use in SLS trajectory simulations.
- 2,000 seasonal one-hour quintuplets to examine launch window effects.

- Wind pairs to support NASA's Launch Services Program (Decker and Barbré 2014).
- 2,000 seasonal winds including measurements from a local 500-ft tower for ground wind applications.

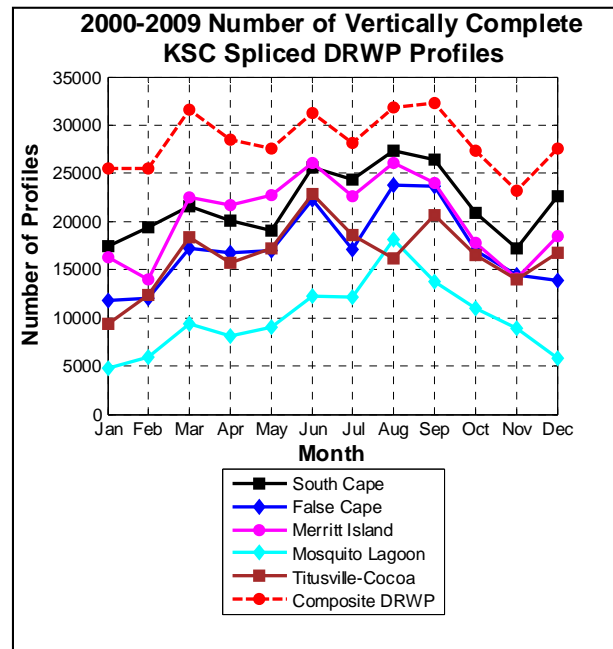


**Figure 16:** Number of available spliced DRWP profiles containing continuous data from 0.25-18.45 km during each month from 2000-2009. Solid lines show the number of spliced profiles generated from an individual 915-MHz DRWP and the 50-MHz DRWP, and the dashed-red line shows the number of composite profiles.

## 8. SUMMARY

This paper describes in detail the QC and splicing methodology for KSC's 50- and 915-MHz DRWP measurements that generates an extensive archive of vertically complete profiles from 0.20-18.45 km. The concurrent POR from each archive extends from April 2000 to December 2009. MSFC NE applies separate but similar QC processes to each of the 50- and 915-MHz DRWP archives. DRWP literature and data examination provide the basis for developing and applying the automated and manual QC processes on both archives. Depending on the month, the QC'ed 50- and 915-MHz DRWP archives retain 52-65% and 16-30% of the possible data, respectively. The 50- and 915-MHz DRWP QC archives retain 84-91% and 85-95%, respectively, of all the available data provided that data exist in the non-QC'ed archives. Next, MSFC NE applies an algorithm to splice concurrent measurements from both DRWP sources. Last, MSFC NE generates a composite profile from the (up to) five available spliced profiles to effectively characterize boundary layer winds and to utilize all possible 915-MHz DRWP measurements at each timestamp. During a given month, roughly 23,000-32,000 complete profiles exist from 0.25-18.45 km from the

composite profiles' archive, and approximately 5,000-27,000 complete profiles exist from an archive utilizing an individual 915-MHz DRWP. One can extract a variety of profile combinations (pairs, triplets, etc.) from this sample for a given application.

The sample of vertically complete DRWP wind measurements not only gives launch vehicle customers greater confidence in loads and trajectory assessments versus using balloon output, but also provides flexibility to simulate different DOL situations across applicable altitudes.

In addition to increasing sample size and providing more flexibility for DOL simulations in the vehicle design phase, the spliced DRWP database provides any upcoming launch vehicle program with the capability to utilize DRWP profiles on DOL to compute vehicle steering commands, provided the program applies the procedures that this report describes to new DRWP data on DOL. Decker et al. (2015) details how SLS is proposing to use DRWP data and splicing techniques on DOL. Although automation could enhance the current DOL 50-MHz DRWP QC process and could streamline any future DOL 915-MHz DRWP QC and splicing process, the DOL community would still require manual intervention to ensure that the vehicle only uses valid profiles. If a program desires to use high spatial resolution profiles, then the algorithm could randomly add high-frequency components to the DRWP profiles. The spliced DRWP database provides lots of flexibility in how one performs DOL simulations, and the algorithms that this report provides will assist the aerospace and atmospheric communities that are interested in utilizing the DRWP.

## 9. REFERENCES

- 45<sup>th</sup> Space Wing: 2013. Eastern Range Meteorological Handbook: 915 MHz DRWP. [Contact 45SW Public Affairs online at <http://www.patrick.af.mil/main/contactus.asp> for document access].
- Barbré Jr., R.E., 2012: Quality Control Algorithms for the Kennedy Space Center 50-MHz Doppler Radar Wind Profiler Winds Database. *J. Atmos. Oceanic Technol.*, 29, 1731–1743.
- Barbré, Jr., R. E., "Characteristics of the Spliced KSC Doppler Radar Wind Profiler Database". Jacobs ESSSA Group Analysis Report. ESSSA-FY13-1935. November 2013.
- Carr, F.H., P. L. Spencer, C. A. Doswell, and J. D. Powell. 1995: A Comparison of Two Objective Analysis Techniques for Profiler Time–Height Data. *Mon. Wea. Rev.*, 123, 2165–2180.
- Decker, R. K. and R. E. Barbré Jr. 2011: Quality Control Algorithms and Proposed Integration Process for Wind Profilers Used by Launch Vehicle Systems. Paper presented at the 15<sup>th</sup> Conference on Aviation, Range, and Aerospace Meteorology. American Meteorological Society. Los Angeles, California. 3 Aug 2011.
- Decker, R. K. and R. E. Barbré Jr. 2014: Temporal Wind Pairs for Space Launch Vehicle Capability Assessment and Risk Mitigation. *Journal of Spacecraft and Rockets*. doi <http://arc.aiaa.org/doi/abs/10.2514/1.A33000>.
- Decker, R. K., R. E. Barbre, Jr., R. Leach, J. R. Walker, and J. C. Brenton. Assimilation of Wind Profiles from Multiple Doppler Radar Wind Profilers for Space Launch Vehicle Applications. Paper presented at the 19<sup>th</sup> Conference on Integrated Observing and Assimilation Systems for the Atmosphere, Oceans, and Land Surface. American Meteorological Society. Phoenix, Arizona. 8 Jan 2015.
- Lambert, W. C., F. J. Merceret, G. E. Taylor, and J. G. Ward: 2003. Performance of Five 915-MHz Wind Profilers and an Associated Automated Quality Control Algorithm in an Operational Environment. *J. Atmos. Oceanic Technol.*, 20, 1488–1495.
- Lambert, W. C., and G. E. Taylor: 1998. Data Quality Assessment Methods for the Eastern Range 915 MHz Wind Profiler Network. NASA Contractor Report CR-1998-207906, Kennedy Space Center, FL, 49 pp. [Available from ENSCO, Inc., 1980 N. Atlantic Ave., Suite 230, Cocoa Beach, FL, 32931.]
- Leahy, F. B., and B. G. Overbey: 2004. An Analysis of the Automated Meteorological Profiling System Low Resolution Flight Element. Proc. 42nd AIAA Aerospace Sciences Meeting and Exhibit, Reno, NV, AIAA, AIAA-2004-908.
- Leslie, F. W. and C. G. Justus: 2011. The NASA Marshall Space Flight Center Global Reference Atmospheric Model – 2010 Version. NASA/TM—2011–216467. Huntsville, AL.
- Merceret, F. J.: 1997. Rapid Temporal Changes of Midtropospheric Winds. *J. Appl. Meteor.*, 36, 1567–1575.
- Merceret, F. J.: 2000. The Coherence Time of Midtropospheric Wind Features as a Function of Vertical Scale from 300 m to 2 km. *J. Appl. Meteor.*, 39, 2409–2420.
- Murri, D.G.: 2011. Doppler Radar Profiler for Launch Winds at the Kennedy Space Center (Phase 1a). NASA/TM-2011-217321. NESC-RP-11-00692. NASA / LaRC / NESC. Hampton, VA.
- Pinter, D. J., F. J. Merceret, and C. V. Hatley: 2006. Performance Validation of Upgraded Eastern Range 50-Megahertz Doppler Radar Wind

- Profiler. J. Spacecr. Rockets, 43, 693– 695.
- Radian International: 2001. LAP®-3000 Operation and Maintenance Manual. Document Control 80018201, Revision F, 376 pp.
- Richards, J. A.: 1993. Remote Sensing Digital Image Analysis: An Introduction. Springer -Verlag, 340 pp.
- Rinehart, R. E.: 2004. Radar for Meteorologists. 4th ed. Rinehart Publications, 482 pp.
- Schumann, R. S., G. E. Taylor, S. A. Smith, and T. L. Wilfong: 1995. Application of 50-MHz Doppler Radar Wind Profiler to Launch Operations at Kennedy Space Center and Cape Canaveral Air Station. Preprints, 14th Conf. on Weather Analysis and Forecasting, Dallas, TX, Amer. Meteor. Soc., 428–433.
- Taylor, G. E., J. T. Manobianco, R. S. Schumann, M. M. Wheeler, and A. M. Yersavich: 1993. Final Report on the Implementation and Evaluation of the New Wind Algorithm in NASA's 50 MHz Doppler Radar Wind Profiler. NASA Applied Meteorology Unit Contractor Rep. 194880, 138 pp. [Available online at <http://science.ksc.nasa.gov/amu/final-reports/drwp-algorithm.pdf>.]
- Wilfong, T. L., S. A. Smith, and R. L. Creasey: 1993. High Temporal Resolution Velocity Estimates From a Wind Profiler. J. Spacecr. Rockets, 30, 348–354.